Matter-Wave Decoherence due to a Gas Environment in an Atom Interferometer

Hermann Uys, John D. Perreault, and Alexander D. Cronin
Department of Physics, University of Arizona, Tucson, Arizona 85721, USA
(Received 9 February 2005; published 5 October 2005)

Decoherence due to scattering from background gas particles is observed for the first time in a Mach-Zehnder atom interferometer, and compared with decoherence due to scattering photons. A single theory is shown to describe decoherence due to scattering either atoms or photons. Predictions from this theory are tested by experiments with different species of background gas, and also by experiments with different collimation restrictions on an atom beam interferometer.

DOI: 10.1103/PhysRevLett.95.150403 PACS numbers: 03.75.−b, 03.65.Yz, 39.20.+q

When a quantum system in a superposition of states interacts with an environment, the coherence of the superposition can be lost. Modern decoherence theory explains this is a result of entanglement between the system and unobserved degrees of freedom in the environment [1]. Understanding how different environments cause decoherence is important for applications such as atom interferometry or quantum computation, where coherent superpositions are required.

In this Letter we compare two different mechanisms for decoherence: scattering atoms and scattering light. A dilute gas of massive particles and a beam of radiation are quite different environments, yet they both cause contrast loss in our atom interferometer. The data and analysis presented here show that *gas decoherence* (atom scattering) and *photon decoherence* (light scattering) can be understood with a single universal theory described by Tan and Waals [2] and also Tegmark [3]. Motivated by this theory, we show that the distribution of momentum transfer from the environment to the *detected* atoms determines the amount of contrast loss regardless of the kind of objects being scattered in the environment.

To study gas decoherence, we vary the background pressure in the entire interferometer chamber while monitoring the transmitted flux, as well as the interference contrast which we define as $C = (I_{\max} - I_{\min})/(I_{\max} + I_{\min})$, where $I_{\max(\min)}$ is the maximum (minimum) count rate in the interference fringes. The presence of contrast reflects the fact that the atoms are in a coherent superposition of states. A related issue is the attenuation of atom beam intensity by the environments. The attenuation is the same on both paths of the interferometer and is therefore equal to the attenuation of the average detected intensity, $\langle I \rangle = (I_{\max} + I_{\min})/2$. In what follows we denote the contrast and intensity in the absence of scattering by C_0 and I_0. Because the room temperature background gas atoms have more momentum than photons by a factor of $\simeq 10^5$, they can deflect beam atoms by large enough angles that they often miss our detector. As a result, the gas environment reduces the average atom beam intensity to 10% before the contrast is halved. By comparison photon scattering does not reduce the detected flux (see Fig. 1).

One can compare the two environments as two gedanken microscopes that use either light waves or de Broglie waves of background gas to detect which path atoms took in the interferometer. According to Feynmann's Heisenberg microscope idea [4], a quantum system can be localized with a spatial resolution δx of

$$\delta x \geq \frac{\lambda}{2\mathrm{NA}} = \frac{h}{2p\mathrm{NA}}, \tag{1}$$

where λ is the wavelength of the light or the wavelength of the gas particles used to make the microscope, p is the momentum of the photons (or gas particles), and NA is the numerical aperture of the microscope. The inequality in Eq. (1) becomes an equals sign if the microscope is limited only by diffraction. Heuristically, by detecting an atom's position the microscope can observe the particle nature of an atom, which is complementary to the wave nature. Hence, if such a microscope can even in principle resolve which path each atom took in the interferometer, then evidence for the wave nature of atoms (i.e., the interference fringe contrast) should be unobservable.

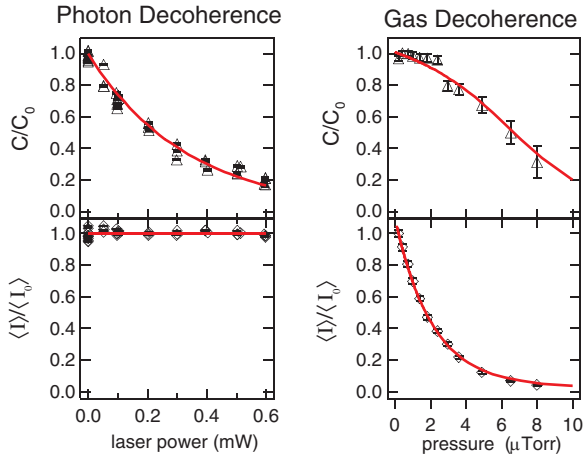

FIG. 1 (color online). Comparison of photon decoherence (left) to gas decoherence (right). Contrast and intensity in an atom beam interferometer are reported as a function of resonant laser beam power or background gas pressure. The curves come from a general theory of decoherence given by Eqs. (2) and (3).

 © 2005 The American Physical Society

Since the gedanken gas microscope has a smaller wavelength probe than the light microscope, it is natural to expect that gas scattering should cause more contrast loss than photon scattering. In apparent contradiction to this simple picture, the contrast is not destroyed even when there is a sufficient gas pressure to attenuate the atom beam. As we shall explain, the analysis of the gedanken microscope resolution must be adjusted to include the probability distribution of momentum kicks from the environment to each detected atom, and in the case of the gas environment this leads to poorer gedanken microscope resolution than predicted by the ideal limit.

Our experiment employs a Mach-Zehnder atom interferometer, shown in Fig. 2, with two arms formed by the zeroth and first diffraction orders of a supersonic Na atom beam (mean velocity 3000 m/s and $\Delta v/\langle v\rangle \approx 1/10$) that passes through a 100 nm period grating. A second grating redirects the beams so they overlap and make flux density interference fringes at the position of a third grating. Atoms transmitted through the third grating are detected with a hot wire, and oscillations in the flux due to the interference contrast are observed when the third grating is translated. At a background gas pressure of 2×10^{-7} Torr, the contrast is $C_0 \simeq 25\%$ and the average detected atom flux is $I_0 \simeq 100\,000$ counts per second. The beam is collimated to 2×10^{-5} rad by two 10 μm slits separated by 1 m, and the detector is 50 μm in diameter. The gratings are each separated by 1 m. To study gas decoherence, we vary the background pressure by controlling a gas leak into the interferometer chamber while monitoring the beam intensity and interference contrast. Note that the entire interferometer chamber is filled with gas so scattering can take place anywhere along either arm of the interferometer. This setup is different from atom interferometer experiments in which a gas cell was placed on one arm [5] or from neutron interferometer experiments with an absorbing structure in one arm [6]. Those cases lead to attenuation in one arm only. In our case both arms are exposed to the same gas environment and experience the same attenuation. (We discuss gas decoherence in relation to [5,6] more in the conclusion).

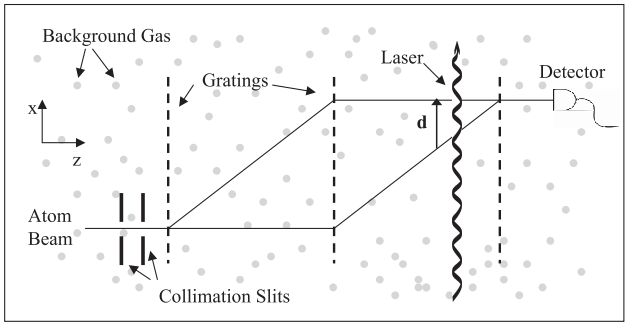

FIG. 2. Schematic of the atom interferometer and scattering scenarios. For gas decoherence the entire interferometer is exposed to background gas, allowing scattering to take place anywhere along both arms of the interferometer. Previous experiments [7–9] studied photon scattering from the two arms at a location where the separation vector **d** is defined.

Our apparatus was previously used to study photon decoherence [7–10]. That experiment used a laser beam tuned to the $\lambda = 590$ nm transition of the Na beam atoms that was positioned as indicated in Fig. 2, so as to scatter off of both arms of the interferometer. The contrast was monitored as a function of laser intensity and as a function of the separation vector, **d**, between the two arms of the interferometer at the location of scattering. This Letter is the first report of gas decoherence in a Mach-Zehnder interferometer. A Talbot Lau interferometer was used recently to study gas decoherence [11], but our observations are in a different regime since the momentum spread of our detected beam is 10 000 times smaller than in the Talbot Lau interferometer [12]. Unlike [11] we do not get an exponential decay of contrast with gas pressure (see Fig. 1). It was also suggested in [11] that gas decoherence could not be observed in our Mach-Zehnder interferometer because all the scattered atoms would miss the detector. Indeed, in the limit of an infinitely narrow beam and detector, only atoms with zero recoil could be detected. In that case the momentum transfer, $(p\mathrm{NA}) = 0$, so by Eq. (1) a Heisenberg microscope would have poor resolution and fringe contrast could therefore be preserved. We attribute the possibility of gas decoherence in our apparatus to the nonzero size of the atom beam and the detector. To confirm this, we present data showing that gas decoherence depends on the beam collimation in Fig. 3.

Figure 3(a) compares the contrast loss, C/C_0, observed as a function of the average beam intensity, $\langle I\rangle/\langle I_0\rangle$, when different species of background gas (Xe, Ar, He, and N_2) are introduced to the interferometer chamber. These data form a universal curve even though quite different amounts of pressure are needed for each gas to cause a 50% reduction in atom beam intensity. Figure 3(b) shows similar data obtained with wider collimating slits. The solid and dashed lines come from our decoherence theory described next.

The results of Fig. 3 can be understood within a widely accepted picture of decoherence that views every system as a subset of a larger environment that is also governed by quantum mechanics, but is not monitored by the observer [1]. The result of coupling to this environment is that the off-diagonal elements of the density matrix describing the system are damped. This picture was successfully used to explain the photon decoherence experiment [7–10] in which case the damping of off-diagonal elements of the density matrix causes a reduction in contrast to $C = \beta C_0$. The *decoherence function,* β, is

$$\beta(\mathbf{d}) = \frac{\int_{\Delta k_{\min}}^{\Delta k_{\max}} P(\Delta\mathbf{k}) e^{-i(\Delta\mathbf{k})\cdot\mathbf{d}} d\Delta\mathbf{k}}{\int_{\Delta k_{\min}}^{\Delta k_{\max}} P(\Delta\mathbf{k}) d\Delta\mathbf{k}}, \qquad (2)$$

as predicted by [2,3]. In Eq. (2), $P(\Delta\mathbf{k})$ is the probability distribution to undergo a momentum change $\hbar\Delta\mathbf{k}$ due to

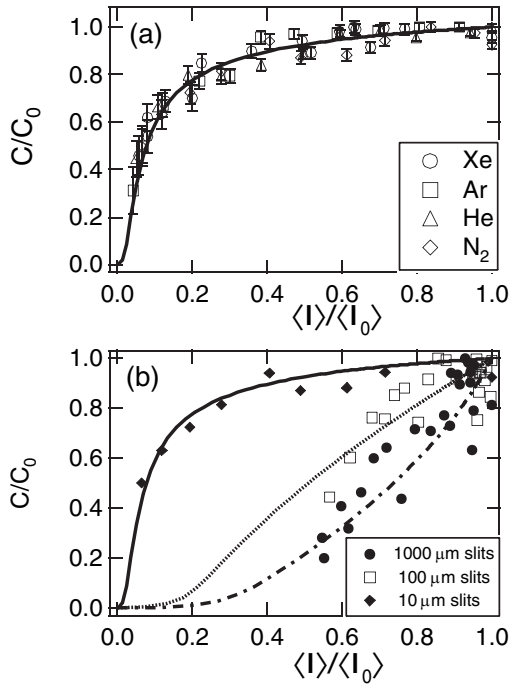

FIG. 3. Contrast and intensity shown in parametric plots as a function of the pressure of the background gas. (a) Various background gas species provide similar results. (b) Large atom beams cause more rapid loss of contrast. Theory curves are from Eqs. (4) and (5).

scattering. The limits of integration are determined by $\Delta\mathbf{k}_{\max(\min)}$ that still permit the atom beam to be detected. The denominator simply expresses the total probability, P_{det}, for a beam atom to be detected. We emphasize that $\Delta\mathbf{k}_{\max(\min)}$ depends not only on the size of the detector, but also on the initial position and momentum of the beam atoms. To find β, one must therefore average over the beam width and height.

To describe $P(\Delta\mathbf{k})$, one must take into account the probability, P_n, that an atom undergoes exactly n scattering events on its trajectory to the detector plane. P_n is determined by the background gas pressure or radiation intensity. $P(\Delta\mathbf{k})$ also depends on the probability that the atom gets a total momentum kick $\Delta\mathbf{k}$ as a result of these n scattering events. This is given by the convolution (which we indicate with $*$) of the absolute value squared of the scattering amplitude $f \equiv f(\Delta\mathbf{k})$ with itself n times, because the probability distribution function of two random variables is the convolution of the constituent distribution functions. We write

$$P(\Delta\mathbf{k}) = P_0\delta(\Delta\mathbf{k}) + \left(P_1\frac{|f|^2}{\sigma_t} + P_2\frac{|f|^2 * |f|^2}{\sigma_t^2} + \ldots\right), \tag{3}$$

where $\delta()$ is the Dirac delta function, and f is explicitly normalized by the total scattering cross section σ_t.

In practice we account for the averaging over beam profile in Eq. (2) in an approximate way by multipying the term in brackets on the right in Eq. (3) (i.e., terms accounting for multiple scattering) by $(1 + \frac{A_{\text{beam}}}{A_{\text{det}}})$, where A_{beam} is the cross-sectional area of the beam and A_{det} the cross-sectional area of the detector. The weight factor $\frac{A_{\text{beam}}}{A_{\text{det}}}$ then allows for the possibility that beam atoms that would have missed the detector in the absence of scattering, might now be scattered onto the detector.

Up to this point, the theory used in Eqs. (2) and (3) is still general enough to describe both photon decoherence and gas decoherence. Indeed, this universal model of decoherence from scattering serves as the basis for all the theoretical curves presented in Figs. 1 and 3. For the photon environment, P_n and $|f(\Delta k)|^2$ are determined by atom-photon interactions, e.g., dipole radiation scattering as discussed in [7–10]. For the gas environment it can be shown that the probability to scatter n times after traveling a distance z through the background gas obeys the Poisson distribution $P_n = \frac{z^n}{n!\,\lambda^n}e^{-z/\lambda}$, where λ is the mean free path. Furthermore $f(\Delta k)$ is the complex amplitude of an outgoing spherical wave in the Lippman-Schwinger equation, which in the Born approximation is simply the Fourier transform of the interatomic potential [13].

A thorough calculation of the decoherence function for the gas environment should also include an average over initial momentum states of the background gas. The main effect of the averaging procedure described by Russek [14] is to scale the scattering angle in the laboratory, θ, with respect to that in the center of mass frame, Θ, according to $\theta \approx \frac{m_g}{m_g+m_b}\Theta$ where m_g is the mass of the background gas atom and m_b the mass of the beam atom. This approximation is valid when the atom beam speed is large compared the average speed of the background gas atoms, and it was used in this analysis to find $f(\Delta\mathbf{k})$.

Since scattering from the background gas can take place anywhere along the interferometer, the decoherence function should also be averaged over $\mathbf{d}$. However, instead of explicitly averaging over $\mathbf{d}$, we note that terms in the numerator of the decoherence function, Eq. (2), are small if they oscillate rapidly over the range of integration, i.e., when $\mathbf{d}\cdot\Delta\mathbf{k} > 2$. For gas scattering this rapid oscillation of the integrand occurs for values of $\mathbf{d}$ corresponding to scattering a distance of $z \geq 1$ mm from the third (or first) grating. Therefore only scattering that takes place close to the third (or first) grating gives significant contributions to β. The consequence of averaging over $\mathbf{d}$, which we indicate with angle brackets, is therefore that to a good approximation *only atoms that do not scatter contribute coherently to the interference pattern.* With this consideration the predicted contrast based on Eqs. (2) and (3) reduces to

$$\langle C\rangle_d \approx C_0\left\langle\frac{P_0}{P_{\text{det}}}\right\rangle_d, \tag{4}$$

and the detected flux is

$$\langle I\rangle_d \approx I_0\langle P_{\rm det}\rangle_d. \quad (5)$$

These predictions show good agreement with experimental data as seen in Figs. 1 and 3. Note, in particular, that data taken with the Na atom beam and all background gases tested (He, Ar, Xe, N_2) collapse on the same curve in this plot. This is due to the fact that the spatial extent of the interatomic potential is very similar for Na and all the gases used [the minimum in $V(r)$ is located near 5 Å for each of these gases [15]]. As a consequence, the widths of the scattering probability distributions, $|f(\Delta\mathbf{k})|^2$, are similar for these gases.

Equations (2) and (3), and the Born approximation for $f(\Delta k)$, taken together allow us to predict that faster beams or scattering centers with larger spatial extent to their potential will cause more contrast loss per attenuation, since both of these scenarios lead to narrower $P(\Delta\mathbf{k})$ and hence a larger $P_{\rm det}$. Furthermore, a larger detector or larger atom beam (hence larger $\Delta k_{\rm max}$) will also cause more contrast loss, since this would increase the incoherent contribution to the denominator in Eq. (2) due to scattering.

We have tested one of these predictions by using a beam with a larger cross-sectional area. A wide beam is beneficial for applications such as gyroscopes [16] where high flux is desired, but separated beams are not needed. Figure 3(b) compares the contrast, C/C_0, as a function of atom flux, $\langle I\rangle/\langle I_0\rangle$, for three beam sizes. Note that contrast is diminished more rapidly for the wider beam as predicted by Eqs. (4) and (5). Optimizing interferometer performance for practical applications therefore relies on a tradeoff between desired intensity and contrast at the achievable vacuum levels.

In the vocabulary of related work [6], the gas environment is a stochastic absorber in the quantum limit. Furthermore, as predicted by [6] for an environment such as the gas that interacts with both arms of the interferometer, if only nonscattered atoms were detected then $P_{\rm det} = P_0$ and C/C_0 would remain 1 even as $\langle I\rangle/\langle I_0\rangle$ is reduced to P_0.

As a final point we discuss the impact of gas decoherence on experiments in which the atom wave index of refraction due to a dilute gas was measured [5]. Additional incoherent flux that hits the detector does not affect the fringe phase, nor does it change the product $\langle I\rangle C$. Thus the gas decoherence described here should not influence results reported in [5].

In conclusion, we have observed loss of interference contrast in a Mach-Zehnder atom interferometer as a result of increased background gas pressure. Momentum transfer from the gaseous environment causes decoherence of scattered atoms so that only atoms that undergo no scattering contribute coherently to the interference pattern. These results are explained by a general theory of decoherence that treats gas scattering and photon scattering equally. This theory allows us to predict that higher velocity beams, atoms with longer range potentials, a wider detector, or a wider beam will increase the contrast loss from gas decoherence. This provides quantitative predictions for interferometer performance in imperfect vacuum.

This work was supported by Research Corporation and the National Science Foundation Grant No. 0354947.

[1] W. H. Zurek, Phys. Today **44**, No. 10, 36 (1991); *Quantum Theory and Measurement*, edited by J. A. Wheeler and W. Zurek (Princeton University Press, Princeton, NJ, 1983); W. H. Zurek, Rev. Mod. Phys. **75**, 715 (2003); D. Giulini, E. Joos, C. Kiefer, J. Kupsch, I.-O. Stamatescu, and H. D. Zeh, *Decoherence and the Appearance of a Classical World in Quantum Theory* (Springer-Verlag, Heidelberg, 1996); M. Namiki and S. Pascazio, Phys. Rev. A **44**, 39 (1991).
[2] S. Tan and D. Walls, Phys. Rev. A **47**, 4663 (1993).
[3] M. Tegmark, Found. Phys. Lett. **6**, 571 (1993).
[4] R. Feynman, R. Leighton, and M. Sands, *The Feynman Lectures on Physics* (Addison-Wesley, Reading, MA, 1965), Vol. 3.
[5] J. Schmiedmayer *et al.*, Phys. Rev. Lett. **74**, 1043 (1995); T. D. Roberts, A. D. Cronin, D. A. Kokorowski, and D. E. Pritchard, *ibid.* **89**, 200406 (2002).
[6] J. Summhammer, H. Rauch, and D. Tuppinger, Phys. Rev. A **36**, 4447 (1987); J. Summhammer and H. Rauch, *ibid.* **46**, 7284 (1992).
[7] M. Chapman *et al.*, Phys. Rev. Lett. **75**, 3783 (1995).
[8] *Atom Interferometry*, edited by P. Berman, Advances in Atomic, Molecular, and Optical Physics (Academic Press, San Diego, 1997).
[9] D. Kokorowski *et al.*, Phys. Rev. Lett. **86**, 2191 (2001).
[10] D. Pritchard *et al.*, Ann. Phys. (N.Y.) **10**, 35 (2001).
[11] K. Hornberger *et al.*, Phys. Rev. Lett. **90**, 160401 (2003).
[12] B. Brezger *et al.*, Phys. Rev. Lett. **88**, 100404 (2002).
[13] J. Sakurai, *Modern Quantum Mechanics* (Addison-Wesley, Reading, MA, 1994).
[14] A. Russek, Phys. Rev. **120**, 1536 (1960).
[15] J. Tellinghuisen, J. Chem. Phys. **71**, 1283 (1979); W. Baylis, J. Chem. Phys. **51**, 2665 (1969).
[16] T. L. Gustavson, A. Landragin, and M. A. Kasevich, Classical Quantum Gravity **17**, 2385 (2000).